Article

The First Analysis of Synaptonemal Complexes in Jawless Vertebrates: Chromosome Synapsis and Transcription Reactivation at Meiotic Prophase I in the Lamprey *Lampetra fluviatilis* (Petromyzontiformes, Cyclostomata)

Sergey Matveevsky [1,*], Nikolay Tropin [2], Aleksandr Kucheryavyy [3] and Oxana Kolomiets [1]

[1] Vavilov Institute of General Genetics, Russian Academy of Sciences, Moscow, Russia; sergey8585@mail.ru (SM), olkolomiets@mail.ru (OK)
[2] Vologda branch of the Russian Federal Research Institute of Fisheries and oceanography, Vologda, Russia; nikolay-tropin1@yandex.ru (NT)
[3] Institute of Ecology and Evolution, Russian Academy of Sciences, Moscow, Russia; kucheryavyy@sevin.ru (AK)
* Correspondence: s.matveevsky@vigg.ru (SM)

Abstract: This paper presents results of the experiments performed on a nonconventional and extremely interesting in regard to evolution, creature, the European river lamprey *Lampetra fluviatilis* (Petromyzontiformes, Cyclostomata), one of the oldest taxa of vertebrates. We present detailed immunocytochemical and electron microscopy analyses of chromosome synapsis, the transcription process, and chromatin dynamics in lamprey prophase I, which is the first time for science. We found that not all chromosomes complete synapsis. Rounded structures were detected in chromatin and in some synaptonemal complexes but their nature could not be determined conclusively. An analysis of RNA polymerase II distribution led to the conclusion that transcriptional reactivation in lamprey prophase I is not associated with the completion of chromosome synapsis. Monomethylated histone H3K4 is localized to meiotic chromatin throughout prophase I, and this pattern has not been previously detected in the animals. Thus, the findings made it possible to identify synaptic and epigenetic patterns specific for this group, and to add new pieces of the puzzle to the discussions of the scientific issues under study. The research on lamprey meiotic chromatin and chromosomal dynamics raises many questions leading to new discoveries.

Keywords: lamprey; cyclostome; meiosis; chromosome; chromatin; histone; RNA polymerase II

1. Introduction

Meiosis is a two-stage cell division (reduction division: meiosis I, and equational division: meiosis II) accompanied by a range of chromosomal events, including synapsis, recombination, and two rounds of chromosome segregation, the corollary of which is the formation of haploid gametes. Evolutionary, the meiotic pattern is conserved among eukaryotes [1,2]. More interesting are the differences found among taxa. One of features of meiosis is the presence of an extensive system of structural and functional chromatin changes. The main discoveries in this field have been made on mammals as an example and are reflected in several of the papers referred below.

First, it has been established that a massive rearrangement of three-dimensional chromatin organization occurs in meiosis, implying that chromatin compartmentalization is attenuated to facilitate the expression of spermatogenic genes [3]. Second, prophase I chromatin organization is associated with specific chromosomal interactions that create special nuclear architecture and is due to the formation (between homologous chromosomes) of special skeletal multiprotein structures (synaptonemal complexes; SCs), to the length and type of chromosomes, to centromere features, to the number of

 doi:10.20944/preprints202212.0504.v1

heterochromatin regions, and to the ability to form chromocenters as well as to the connection of telomeric sites with the nuclear envelope through shelterin and LINC complexes [4-6].

Third, transcriptional chromatin activity differs among stages of meiosis. It is noteworthy that concurrently with the above-mentioned chromosomal events, a complex gene expression program unfolds. This program involves the expression of more than 20 thousand transcripts exclusively at different meiotic substages; some of these transcripts are necessary for direct meiotic functioning, and the others for future postmeiotic differentiation [7-10]. It has been shown immunocytochemically that the transcription level is low in leptotene and zygotene, then transcription is reactivated in pachytene, which corresponds to a previously identified sharp switch of global gene expression at this stage [7]. Then, transcription is retained in diplotene and is again suppressed in metaphase I until the end of the second meiotic division [11-13]. Transcriptional activity in prophase I is directly related to changes in chromatin structure, in particular to post-translational modifications of specific nuclear proteins (histones), including acetylation, methylation, phosphorylation, ubiquitination, and sumoylation [14]. For instance, asynaptic regions in early prophase I trigger transcriptional chromatin inactivation (meiotic silencing of unsynapsed chromosomes; MSUC) [15], which involves histone H2AX phosphorylated at serine 139 in response to the formation of DNA double-strand breaks [16-18]. Trimethylated histone H3K9 (H3K9me3) and monomethylated histone H3K4 (H3K4me1) fill the entire nucleus in murine early prophase I, and starting from pachytene, are retained only in specific small areas [12,13, 19], which may indicate their role in meiotic silencing.

Thus, chromatin modification in prophase I is linked with comprehensive programs of gene expression and epigenetic reorganization. The main discoveries in this field have been made on a conventional model: the mouse. Information on the patterns of meiotic transcription and meiotic silencing in other taxa is scarce and fragmentary. Some examples will be given in the Discussion section.

In this paper, in the context of the meiotic processes described above, we present results of our study on a living "fossil": the migratory European river lamprey *Lampetra fluviatilis* Linnaeus, 1758 (Petromyzontiformes, Cyclostomata). Migratory lampreys are eel-shaped facultative hematophagous ectoparasites or predators [20]. They attack various fishes using a large sucker armed with sharp teeth, which surrounds the mouth opening [21]. Agnathans separated from the main branch of the vertebrate evolutionary tree, i.e., jawed vertebrates (gnathostomes), between 535 and 462 million years ago [22-24]. They formed an evolutionarily independent lineage of lower vertebrates with pronounced features of the lifestyle, morphogenesis, embryogenesis, gametogenesis, and genome. Studies on this animal group are of considerable interest in terms of understanding early stages of the vertebrate divergence [25]. In recent years, hagfish and lampreys attracted increasing attention of researchers owing to a breakthrough in the elucidation of the role and mechanisms of elimination of a substantial part of the genome during normal embryonic development [26-28]. Surprisingly, to our knowledge, there is still not a single report on SCs and meiotic processes of the first meiotic prophase in representatives of jawless vertebrates. Here, for the first time, we present detailed immunocytochemical and electron microscopy analyses of chromosome synapsis and transcription in river lamprey prophase I. These experiments allowed us to identify epigenetic patterns specific to this taxon and to add new pieces of the puzzle to the discussion of the scientific issues under study.

2. Materials and Methods

2.1. Lampreys

Four adult males of *L. fluviatilis* (LF-01, LF-02, LF-03 and LF-04) were caught in the Chernaya River near the Karshevo village (Pudozhsky District, Karelia, Russia). The

 doi:10.20944/preprints202212.0504.v1

Chernaya River belongs to the Onega Lake basin. The studied lamprey is a freshwater potamodromous form of *L. fluviatilis* from the eastern part of the species' area.

2.2. Meiotic chromosome studies and immunostaining procedure

SC preparations were made and fixed according to Peters et al., 1997 [29] with modifications [30] for immunostaining and to Kolomiets et al., 2010 [31] for immunostaining and silver nitrate staining.

The slides were washed in PBS. Spreads were blocked with HB (holding buffer: PBS, 0.3% BSA, 0.005% Triton X-100). The slides were incubated overnight at 4°C with primary antibodies: rabbit polyclonal anti-SCP3 (#15093, Abcam, Cambridge, UK), mouse monoclonal anti-SCP3 (#97672, #205846, Abcam) diluted to a concentration of 1:200-1:500 in ADB (Antibody Dilution Buffer: PBS, 3% BSA, 0.05% Triton X-100), mouse anti-RNA polymerase II (RNAP II) (1:200, #5408, Abcam), rabbit anti-H3K4me1 (1:300, #8895, Abcam), mouse anti-phospho-histone H2AX (1:500, #22551, Abcam), mouse anti-fibrillarin (1:200, #4566, Abcam), mouse anti-H3K9me3 (1:100, #6001, Abcam), human anti-centromere antibodies CREST (1:100, #90C-CS1058, Fitzgerald Industries International, Concord, MA, USA) and ACA (1:100, #15-235, Antibodies Incorporated, Davis, CA, USA), both diluted in ADB. The slides were washed in PBS and incubated with goat anti-rabbit Alexa Fluore 488 conjugated antibodies (1:500, Abcam, Cambridge, UK), goat anti-human Alexa Fluore 546 conjugated antibodies (1:200–1:400) and goat anti-mouse Alexa Fluore 555 conjugated antibodies (1:400) at 37 °C for two hours. The slides were washed with PBS, rinsed briefly with distilled water, dried and mounted in Vectashield with DAPI (Vector Laboratories, Burlingame, CA, USA). For some details of immunocytochemistry procedures, see [32,33]. The slides were analyzed with an Axioimager D1 microscope CHROMA filter sets (Carl Zeiss, Jena, Germany) equipped with Axiocam HRm CCD camera (Carl Zeiss), and image-processing AxioVision Release 4.6.3 software (Carl Zeiss, Jena, Germany). Images were processed by Adobe Photoshop CS5 Extended.

2.3. Electron microscopy

The slides were stained with 50% silver nitrate solution in a humid chamber at 56°C for 3 hours. The slides were washed in three or four changes of distilled water and air-dried. The stained slides were observed in a light microscope, suitably spread cells were selected, and plastic (Falcon film) circles were cut out with a diamond tap and transferred onto grids. The slides were examined under JEM 1011 electron microscope.

3. Results

3.1. Lamprey chromosome synapsis

To investigate the events and processes occurring in prophase I, we used immunostaining of marker proteins. Each stage was described in accordance with generally recognized morphological changes in chromosomes [1,12,34,35].

All spreads were prepared from four unpaired whitish testicles from four males of river lampreys and examined under light fluorescent and electron microscopes. Numerous spermatocytes of varying degrees of spreading were observed on all slides. Due to the large number of chromosomes, many meiocytes were not spread out sufficiently, and there was a lot of chromosome overlap.

To analyze the structure and behavior of meiotic chromosomes, immunodetection of the SYCP3 protein (a major protein of axial/lateral elements of the SC) was performed. Different anti-SYCP3 antibodies were used: mouse monoclonal antibodies (Abcam, cat. #97672, #205846) raised against the mouse protein and a rabbit polyclonal antibody (Abcam, cat. #15093) raised against the C-terminus of the human protein. Only the latter yielded a positive specific signal. In leptotene spermatocytes, the SYCP3 signal was

 doi:10.20944/preprints202212.0504.v1

found to be diffusely distributed throughout the nucleus with SYCP3-positive DAPI-negative round-like bodies of various sizes, which are conventionally designated as RLBs (round-like bodies) (Fig. 1A, A'–B, B'). Such a tentative name was given due to the lack of information about their true nature. We employed antibodies to detect the location of fibrillarin—an element of the nucleolar dense fibrillar component—but no specific signals were found. At the end of leptotene, forming SYCP3 axes arose (Fig. 1B, B'). In some axes and SCs, round or oval SYCP3- and DAPI-positive nucleolus-like structures were visible at all substages, which were provisionally named SC-associated structures (SCASs) (Figs. 1B, B', C, C', E, E', F, F', G, G', 2, S1, S2). The chromatin around this structure (on the periphery) stained more intensely than in the central part (Figs. 1C, E, G, S2). Variation of the number of RLBs was wide: from 0 (e.g., Fig. S3) to over 50 (e.g., Fig. 3B). In zygotene, SYCP3 axes gave rise to short and long SC fragments (Fig. 1C, C'), and by the end of zygotene, most of SC bivalents formed (Fig. 1D, D'–E, E'), except for terminal regions of chromosomes with incomplete synapsis, which we designated as asynaptic forks (Figs. 1 E'1, E'2, 2A–C). Such forks also persisted until mid pachytene (Figs. 1F, F', F'1, F'2, 2C). At the beginning of diplotene (Fig. 1G, G'), the chromosomal forks were still present (Fig. 1G'1, G'2); therefore, it is likely that some of the bivalents undergo incomplete synapsis throughout the first prophase. Chromosome desynapsis was terminal for some chromosomes, and interstitial for some others (Fig. 1G'1, G'2). Elimination of the SYCP3 protein from the desynaptic axes proceeded segmentally (as if in small parts disappears from the axes; alternating SYCP3-light and -dark sites) (Fig. 1G'1, G'2). Pachytene and diplotene showed one bivalent each with an SCAS in the central part of the nucleus (Fig. 1F, F', G, G'). Both SCASs and RLBs were AgNO3-positive (Fig. S1).

In prophase I, various configurations of axial elements and SCs were observed. Stand-alone univalents were seen in early and mid pachytene (Fig. 1E', F'). In the single bivalents, lateral elements of different lengths were noted (Figs. 2B2, 3D4). The lateral elements of two different bivalents could combine as if forming a trivalent (Fig. 2B', C), similar to the bicentric trivalent-like SC configurations previously found in the sturgeon *Acipenser transmontanus* [35].

To identify centromeric chromosome regions, antibodies to kinetochore proteins, human CREST, and ACA were used. These antibodies did not give a positive specific signal under different incubation conditions.

3.2. Transcription in the first meiotic prophase in the lamprey

The assay of transcriptional activity was carried out by simultaneous immunostaining of the SYCP3 protein and of phosphorylated RNA polymerase II (RNAPII-CTD-Phospho-Ser5, abbreviated as RNAPII). Differential distributions of the signal throughout prophase I were documented. There was no RNAPII signal in the leptotene (Fig. 3A). In early and mid zygotene, a weak RNAPII signal arose as stand-alone dots of various sizes (Figs. 3B, S2A–C, S3). In late zygotene, the amount of the RNAPII signal slightly increased (Fig. 3C) and became brighter by mid pachytene (Figs. 3D, E, S2D–F, S3). The RNAPII signal

Preprints (www.preprints.org) | NOT PEER-REVIEWED | Posted: 27 December 2022 doi:10.20944/preprints202212.0504.v1

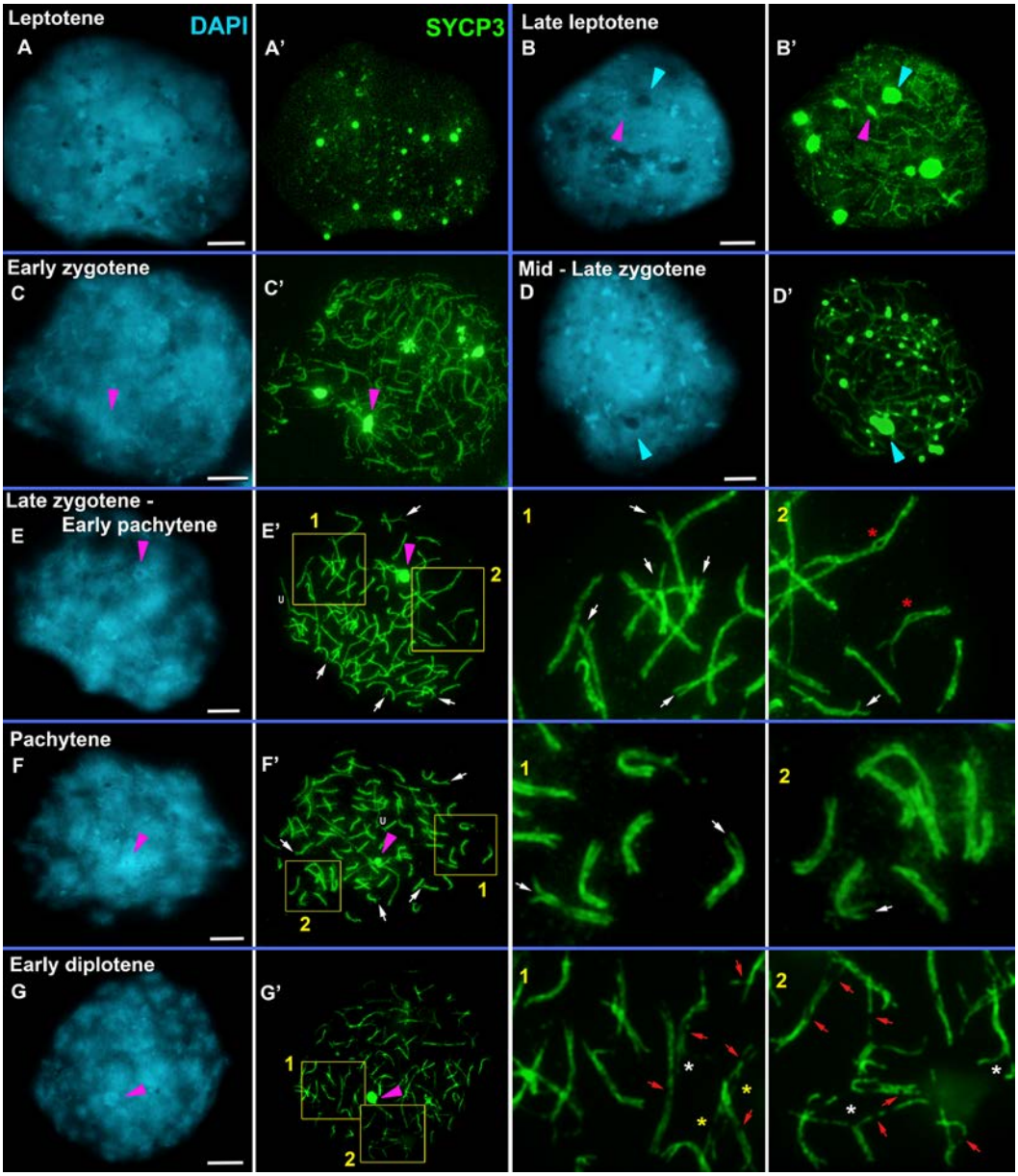

Figure 1. Chromosome synapsis at prophase I in the lamprey. SYCP3 staining (green) revealed the structure and behavior of axial and lateral elements of an SC. DAPI (cyan) stains chromatin. White arrows indicate asynaptic forks in telomeric regions of SC bivalents. Blue arrowheads point to DAPI-negative rounded bodies (RLBs). Pink arrowheads indicate SC-associated rounded structures (SCASs). "U" stands for univalents. **A,A'.** Leptotene. A diffuse SYCP3 signal is distributed throughout the nucleus. Numerous DAPI-negative RLBs of various sizes are seen. **B,B'.** Late leptotene. SYCP3 fragments and axes appear. The diffuse SYCP3 signal is still present throughout the nucleus. Both RLBs and SCASs are present in the nucleus. **C,C'.** Early zygotene (see Fig. S2A–C). Chromosomal axes enter synapsis, forming short and long SC fragments. There is one SCAS in this cell. **D,D'.** Mid–late zygotene. Most of SC bivalents form. Numerous RLBs and SCASs are visible. **E,E'.** Late zygotene to early pachytene. Some bivalents retain short asynaptic interstitial regions (red asterisks). Most bivalents have terminal regions of incomplete synapsis (asynaptic "forks") (E'1, E'2). One of the long SCs has an SCAS in the central part. **F,F'.** Pachytene. Some of the bivalents show complete synapsis, although most of the SCs retain asynaptic "forks" (F'1, F'2). One of long SCs contains an SCAS in the central part. **G,G'.** Early diplotene (see Fig. S2G–I). Desynapsis is accompanied by segment-by-segment removal of the SYCP3 protein from the axes (red arrows). Desynapsis can start from both terminal (white stars) and interstitial (yellow stars) regions of chromosomes (G'1, G'2). Scale bar = 5 μm.

Preprints (www.preprints.org) | NOT PEER-REVIEWED | Posted: 27 December 2022 doi:10.20944/preprints202212.0504.v1

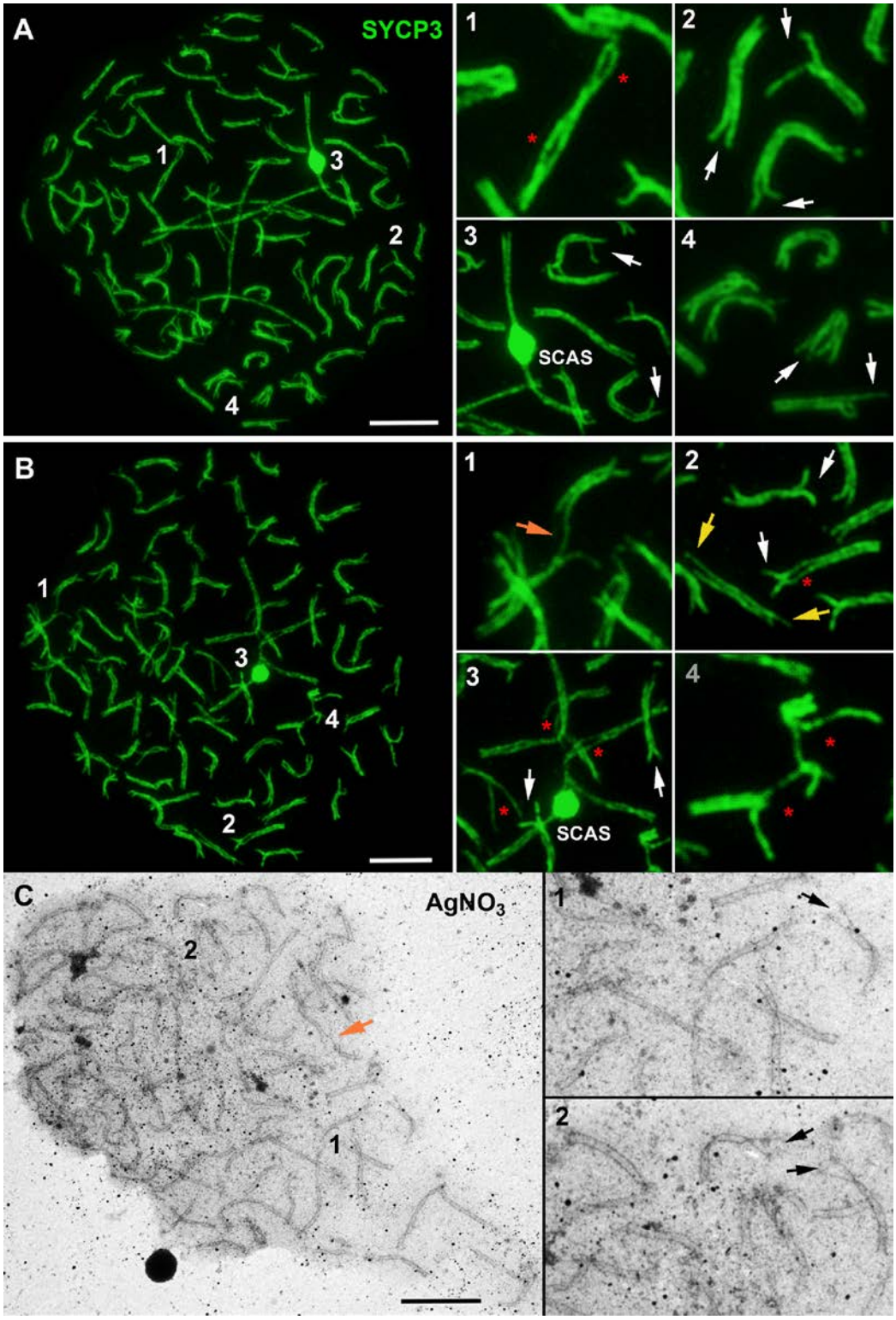

Figure 2. Chromosome synapsis in lamprey spermatocytes at late zygotene to early pachytene (A,B: light microscopy) and mid pachytene (C: electron microscopy). SYCP3 staining (green) revealed the structure and behavior of the axial and lateral elements of an SC. White arrows (for A2–A4 and B2–B4) and black arrows (for C1 and C2) indicate asynaptic forks in telomeric regions of SC bivalents. The orange arrow points to the connection of axial elements of two bivalents, forming a trivalent-like SC configuration. The numbers indicate enlarged parts of the nucleus shown on the right. SCAS: an SC-associated structure in large SCs. Red asterisks indicate interstitial asynaptic sites. Yellow arrows point to different lengths of two axial/lateral elements in one bivalent. Scale bar = 5 μm.

 doi:10.20944/preprints202212.0504.v1

was not specifically associated with unpaired and paired segments, including asynaptic forks (Fig. 3D, E). That is, there was no regular variation of RNAPII points along and around bivalents with completed synapsis or not fully synapsed bivalents (Fig. 3D1, 3D1′–3D4, 3D4′, 3E2, 3E2′, 3H). Thus, the initiation of transcriptional reactivation is not associated with the completion of chromosomal synapsis (Fig. 3H). In diplotene, the RNAPII signal has a pattern similar to that in mid pachytene (Figs. 3F, G, S2D–F, S2G–I). The RNAPII signal is diffusely scattered as dot foci throughout meiotic nuclei (Fig. 3D–G), with occasional denser RNAPII signal clumps (Figs. 3D, G, S2, S3). SCASs tend to have fewer weak RNAPII foci (Fig. 3E1–E1′, 3G1–G1′) or no RNAPII signal at all (Fig. 3D5–D5′, 3F1–F1′), likely indicating either low transcriptional activity or its absence in these structures.

Immunocytochemical examination of the distribution of other proteins related to transcriptional regulation failed to detect specific signals of mouse antibodies against γH2AX and H3K9me3. Species specificity of the antibodies may be the reason for the lack of specificity of immunostaining. The choice of new antibodies, new methodological conditions and approaches may help to determine the localization of these proteins in lamprey meiocytes. It is believed that histone H3K4me1 is associated with transcriptional repression of chromatin [36]. Double immunolabeling with antibodies against SYCP3 and H3K4me1 yielded specific staining. Several weak SYCP3 signals in the form of lumps were visible in preleptotene, and the H3K4me1 signal was very weak (slightly above the background level) (Fig. S4). By late leptotene to early zygotene, the amount of the H3K4me1 signal sharply increased (Figs. 4A–C, S4). In mid zygotene, the H3K4me1 signal was bright (Figs. S4, S6). In leptotene and zygotene, the H3K4me1 signal proved to be monomorphically and diffusely distributed throughout the nucleus (Figs. S4, S6). From the end of zygotene to mid pachytene, the H3K4me1 signal looked like separate more or less intense regions. The more intense H3K4me1 domains were located around an SC, while the less bright ones were situated between SCs (Figs. 4D–F, S5, S6). This was especially noticeable in well-spread nuclei. Some bivalent segments were both H3K4me1-positive and H3K4me1-negative (Fig. 4J). At first, we assumed that this phenomenon was due to the degree of completion of synapsis because the intensity of the H3K4me1 signal was slightly lower in asynaptic areas (Fig. 4F1,1′). Nonetheless, this signal varied along bivalents with complete synapsis and bivalents with asynaptic forks (Fig. 4J1,1′–4J5,5′). Asynaptic forks were either H3K4me1-positive (Fig. 4J3,3′) or H3K4me1-negative (Fig. 4J4,4′, 4J5,5′). The number of diplotens was extremely small. A combination of features such as stand-alone SYCP3 axes, the absence of RLBs and bouquet-like configurations, and a domain-like distribution of H3K4me1 helped us to assign the nuclei to the diplotene stage (Fig. S6).

4. Discussion

It would seem that extensive studies on classic experimental models lead to coherent ideas about various biological processes. By contrast, research on nonmodel and taxonomically distant objects brings some smorgasbord, if not chaos, into this picture. In the context of chromosomal and meiotic studies, the European river lamprey is a non-conventional species that has already helped to clarify details of an interesting process: genome elimination. It has been proven that a large part of the genome and even entire chromosomes specific for germ cells are lost during early stages of embryonic development in the sea lamprey *Petromyzon marinus* [26,27]. In the present work, the analysis of chromosome synapsis and of the transcriptional landscape of prophase I chromatin in the lamprey enabled us to add some new data to the existing concepts of synapsis and transcription.

Preprints (www.preprints.org) | NOT PEER-REVIEWED | Posted: 27 December 2022 doi:10.20944/preprints202212.0504.v1

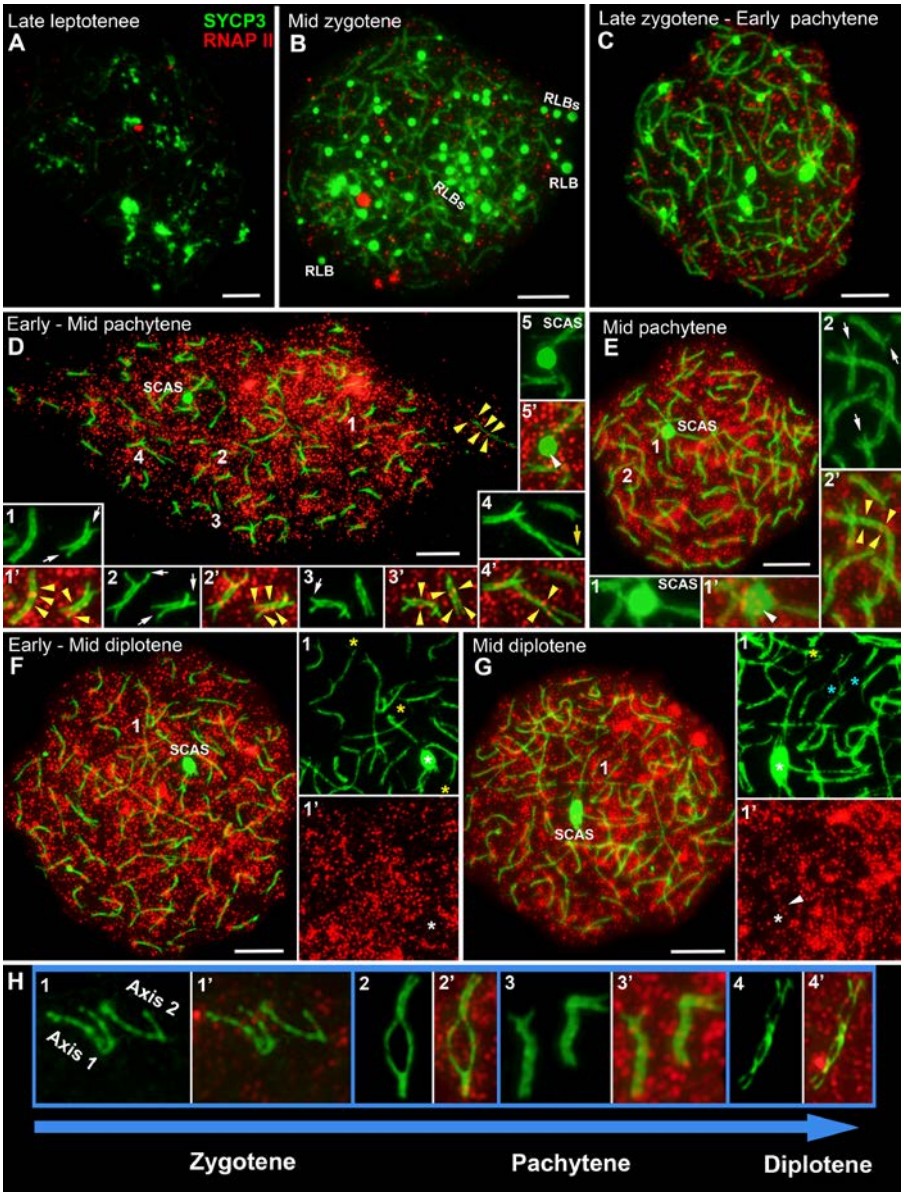

Figure 3. Immunolocalization of the SYCP3 protein (green) and RNA polymerase II (RNAPII, red) in lamprey spermatocytes at different stages of prophase I. White arrows indicate asynaptic forks in terminal regions of bivalents. Yellow arrowheads point to variable localization of RNAPII foci along the synaptic and asynaptic segments of the SC bivalents. SCAS: an SC-associated structure in a long SC. White arrowheads indicate rare stand-alone RNAPII signals within a SCAS. RLB: a round-like body. **A.** Early zygotene. Thin weak SYCP3 axes and SYCP3 lumps of various shapes and sizes are visible. The RNAPII signal is in the form of rare small dots. **B.** Mid zygotene. A large number of RLBs arose throughout nuclear chromatin. The number of rare RNAPII foci of different sizes is greater than that in the previous substage. **C.** Late zygotene to early pachytene. The number of RLBs is less than that in the previous stage. Numerous RNAPII dots, weak in intensity, emerge throughout the nucleus. **D.** Transition from early to mid pachytene. Most of SCs carry terminal asynaptic forks. An intense dot-like pattern of RNAPII signals is seen in the nucleus. The RNAPII signal is distributed unevenly along the bivalents (1, 1'–4, 4'). An SCAS is localized to one of the longest SCs (5). **E.** Mid pachytene. Within an SCAS, there are separate RNAPII foci (1, 1'). Most bivalents have completed synapsis. Nonetheless, many bivalents have asynaptic "forks" (2, 2'). Intense RNAPII foci are noticeable throughout the nucleus. **F, G.** Early and mid diplotene. Desynaptic regions of chromosomes are visible. Some bivalents begin desynapsis from the terminal segments (yellow stars), and others from interstitial segments (blue stars). White asterisks indicate SCASs. Intense RNAPII foci are still present in the nucleus. **H.** Synapsis and desynapsis of some SC bivalents at different stages of prophase I. Scale bars = 5 μm (A–G).

Preprints (www.preprints.org) | NOT PEER-REVIEWED | Posted: 27 December 2022 doi:10.20944/preprints202212.0504.v1

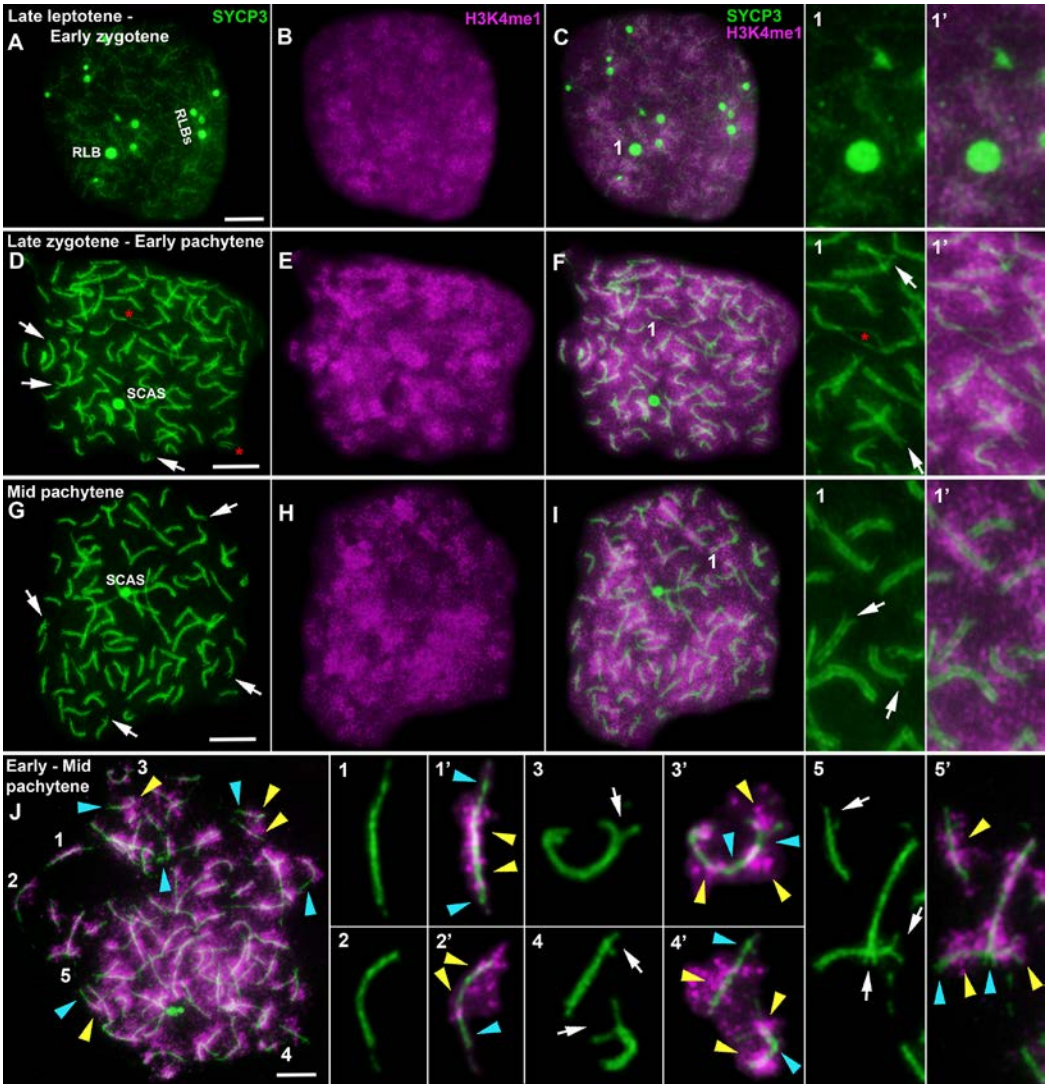

Figure 4. Immunolocalization of SYCP3 (green) and H3K4me1 (magenta) proteins in lamprey spermatocytes at different stages of prophase I. White arrows indicate asynaptic forks in telomeric regions of SC bivalents. Yellow arrowheads point to H3K4me1-positive (enriched) regions of the SCs. Blue arrowheads indicate H3K4me1-negative (not enriched) regions of the SCs. SCAS: an SC-associated structure in a long SC. RLB: a round-like body. **A–C.** Late leptotene to early zygotene. Thin weak SYCP3 axes and SYCP3 lumps of various shapes and sizes are visible. The H3K4me1 signal is evenly distributed throughout the nucleus. The H3K4me1 signal is more monomorphically distributed compared to subsequent stages (1, 1'). RLBs are noticeable in the nucleus. **D–F.** Late zygotene to early pachytene. Zones of interstitial asynapsis in some bivalents or short univalents (red asterisks) are seen (D, 1, 1'). RLBs are absent. The H3K4me1 signal is distributed across the nucleus, but distinct domains with a brighter H3K4me1 signal (E) are present. **G–I.** Mid pachytene. Asynaptic terminal sites are retained in many bivalents (G, 1). Both H3K4me1-positive and H3K4me1-negative domains (H, I, 1, 1') are observed in the nucleus. An SCAS is localized to one of the longest SCs (5). **J.** A well-spread nucleus at the stage of early–mid pachytene. The H3K4me1 signal is distributed within chromatin around SC bivalents. In the SC bivalents, areas with and without a bright H3K4me1 signal (1 1' - 5, 5') are visible. Scale bars = 5 μm (A–J).

4.1. Not all chromosomes show completed synapsis

Few papers are devoted to chromosomes during lamprey meiosis. Robinson and Potter were the first to report on chromosomes during meiosis I in *Mordacia praecox* [37] and *Geotria australis* [38]. Then, meiotic studies contributed to the investigation into the phe-

 doi:10.20944/preprints202212.0504.v1

nomenon of genome elimination in the sea lamprey [27,39]. Until now, however, chromosome synapsis and the processes taking place in chromatin have not been the focus of attention.

The analysis of chromosome synapsis in the river lamprey here made it possible to reveal a number of unusual features. Firstly, we were unable to find a single pachytene nucleus where all the chromosomes showed completed synapsis (instead, there were 6–10 chromosomes without full synapsis). Whether this is a species-specific feature or the stage of completed synapsis is still in progress remains to be clarified. We can theorize that such a stage may be very brief; accordingly, we were unable to identify it. Be that as it may, a very similar case has been observed in the sturgeon *A. transmontanus* [35]. Although those authors did not emphasize this phenomenon, none of the presented spreads contained chromosomes with fully completed synapsis (asynaptic forks were present). It seems that the presence of asynaptic regions at pachytene should lead to pachytene arrest [40-43]. This pattern was discovered in mammals but has not been experimentally confirmed in other vertebrate taxa. In chickens with chromosomal asynapsis due to heterozygosity for translocations, no impairment of spermatogenesis has been detected [44]. Of note, triploid Darevskia lizards with pronounced chromosome asynapsis form spermatozoa but with morphological aberrations in the vast majority of them [45]. The latter observation confirms the notion that the absence of a pachytene checkpoint may underlie the formation of polyploid species [46]. This notion may explain to some extent the terminal segments of asynapsis in the paleotetraploid sturgeon [35]. Probably, the presence of asynaptic forks in lamprey SC bivalents does not prevent further meiocyte progression, which may be due to the absence of the pachytene checkpoint or its nonstandard functioning.

Secondly, trivalent-like SC configurations were found in the lamprey, which also unites them with the sturgeon [35]. Those authors call them bicentric gap configurations and believe that such nuclei can be aneuploid. The similarity in behavior between lamprey and sturgeon meiotic chromosomes seems to be no accident because they share a high diploid number (with macro- and minichromosomes). It cannot be ruled out that the possible paleoploid origin of the karyotype of both species may contribute to such synaptic patterns.

Thirdly, we documented the presence of special bodies called RLBs and SCAS. The first idea that comes to mind is that RLBs may be a morphological manifestation of hypothetical chromatin elimination because outwardly similar micronuclei have been identified during early embryogenesis in the sea lamprey [47]. Nevertheless, these meiotic bodies were DAPI-negative and therefore unlikely to be related to chromatin and probably do not have a nucleolar nature (negative fibrillarin immunostaining). Most likely, these structures are transcriptionally inactive because only rare dim dot-like "transcriptional" signals were present in them, just as within SCASs. An SCAS emits a more intense DAPI signal at the periphery than in the center. At the same time, both types of bodies proved to be subject to silver staining. Thus, the events and structures in prophase I of the river lamprey both share some similarities with sturgeons and possess a series of unique features.

4.2. Lamprey prophase I is characterized by some unique epigenetic patterns

Remodeling and modification of histones during meiosis are processes of a complex epigenetic regulatory system that determines the active or silent state of chromatin. It has been assumed that asynaptic chromatin is a subject to transcriptional silencing [15], and the completion of chromosomal synapsis and repair of DNA double-strand breaks lead to the resumption of transcription, which is reflected in the "synapsis or silencing" model [48]. Later, it was found that a more complex epigenetic program exists in prophase I because transcriptional reactivation does not begin immediately after the completion of synapsis [12]. To determine the activity of transcription at different stages

Preprints (www.preprints.org) | NOT PEER-REVIEWED | Posted: 27 December 2022 doi:10.20944/preprints202212.0504.v1

of lamprey prophase I, we tested RNAPII activity. This type of polymerase is the central coordinator of transcription machinery. Phosphorylation of the C-terminal domain (CTD) of RNAPII regulates and coordinates transcription and chromatin remodeling and modifications [49-51]. We used antibodies to the RNAPII CTD phosphorylated at serine 5 in tandem repeated heptapeptides YSPTSPS. In the lamprey, transcription reactivation begins in early-to-mid zygotene, when the first RNAPII immunosignals arise, and sharply increases toward the beginning of pachytene. This transcription pattern differs from that previously identified in mammals, where reactivation starts in mid pachytene [12,13,52,53]. We propose that transcriptional reactivation in lamprey prophase I is not connected with the completion of chromosome synapsis. The same conclusion was made earlier in a meiotic study on true bugs [54]. Those authors believe that the absence of some repressive chromatin modifications in early prophase I may be responsible for the earlier reactivation. Given that we failed to detect γH2AFX and H3K9me3, we can assume that this hypothesis is applicable to the lamprey. On the other hand, the absence of transcription in leptotene and early zygotene must be explained by some repressive chromatin mechanisms. It is likely that there are some other histone modifications or processes that ensure the silent state of chromatin. This topic requires further research.

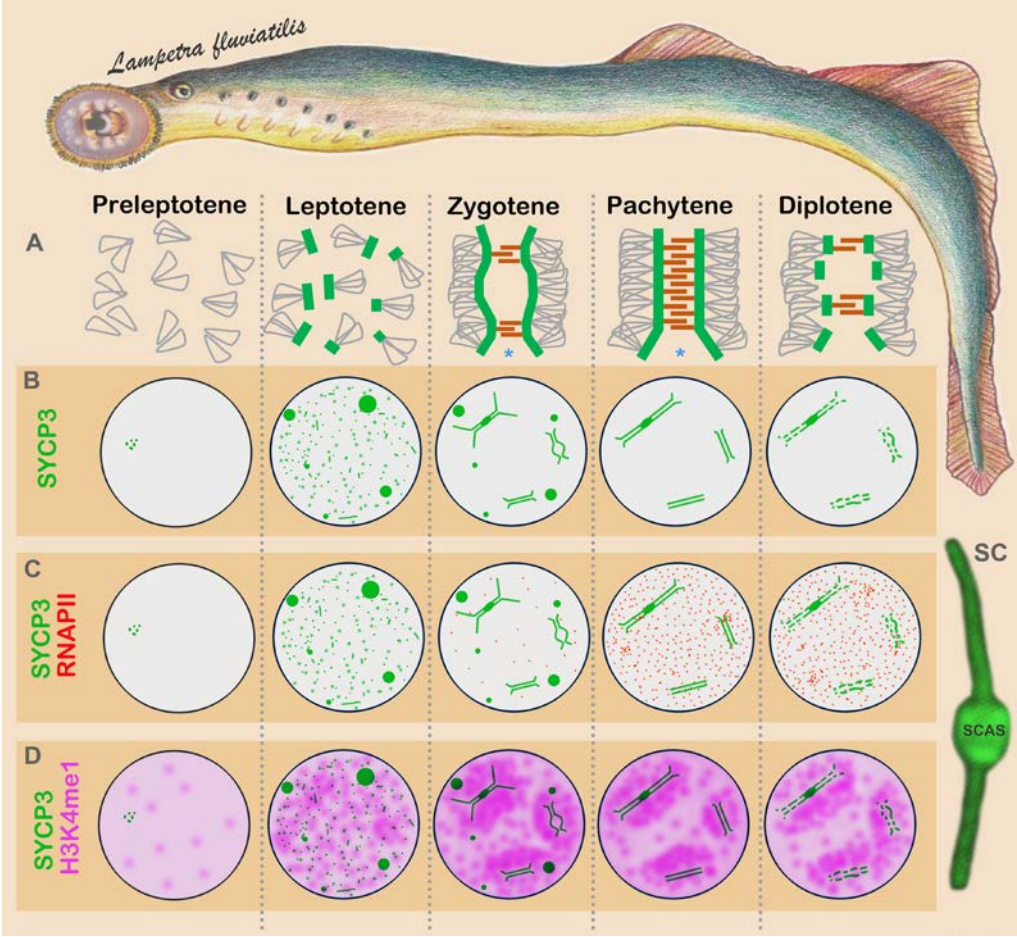

Figure 5. The meiotic first prophase in European river lamprey *Lampetra fluviatilis*. This scheme reflects the features of chromosome synapsis and distributions of some chromatin markers but does not show specifics of the interaction between SCs and the nuclear envelope. SCAS - SC-associated structure. **A.** Schematic representations of SCs at different prophase I substages. The green thick lines represent the lateral elements. The brown lines imitate transverse filaments of the central element of an SC. The gray lines depict chromatin loops. The blue asterisks denote telomeric asynaptic forks. **B.** Dynamics of axial or lateral (SYCP3) elements of SCs. **C.** Dynamics of SCs and of a transcriptional marker (RNAPII). **D.** Dynamics of SCs and of the H3K4me1 histone.

 doi:10.20944/preprints202212.0504.v1

Our results on the H3K4me1 histone distribution in lamprey prophase I are no less intriguing. From leptotene to diplotene (inclusively), an intense H3K4me1 signal was observed throughout the meiotic nucleus with one specific feature: the further the progression of prophase I, the more clustered was histone localization. This distribution differs from what has previously been registered in wild mice [12,13,19]. Because the amount of H3K4me1 diminishes in mid pachytene during mouse meiosis, it has been proposed that this histone is related to silencing [12], especially because a more aberrant H3K4me1 pattern is seen in the sex body of mutant meiocytes [19]. In the case of the lamprey, however, during the transition to the active transcriptional state of chromatin in mid-to-late zygotene, the amount of H3K4me1 stayed unchanged (did not decrease or increase). These findings suggest that H3K4me1 is probably not involved in the cycle of inactivation–reactivation of transcription. Notably, recent research in murine and human germ cells suggests that H3K4me1 may help to implement a transcriptionally neutral gene state that could be activated [55]. It has also been reported that the H3K4me1 histone in somatic cells in the absence of the trimethylated form of H3K4 may correlate with gene repression; on the other hand, this histone has been detected in active gene promoters flanking H3K4me3 [36]. According to the reasoning of Bae and Lesch [55], H3K4me1 may play a context-dependent role in transcriptional regulation.

The function of the H3K4me1 histone in lamprey prophase I remains unknown. Moreover, in well-spread meiocytes, H3K4me1 it was found to be differentially distributed along the SC, suggesting that it can label regions related to different chromatin conformations. High-resolution microscopy has enabled some authors to identify distinct actively transcribed (H3K4me3-positive, loop-like) and repressed (H3K27me3-positive) clusters along pachytene chromosomes [56]. The alternation of H3K4me1-positive and -negative loop-like clusters in lamprey meiotic chromosomes (regardless of synapsis completion) may be due to some kind of chromatin state (possibly transcriptionally neutral) that is not directly connected to transcription but definitely neither prevent this process, nor does it preclude repression in early prophase I. A clear picture of the functions of H3K4me1 in meiotic chromatin is gradually coming into focus.

5. Conclusions

The epigenetics of meiosis is still at the active stage of research, and the discovery of new data helps to get closer to a more complete picture of the functioning of various processes, such as transcription, silencing, and chromatin modification/remodeling. Here, in the European river lamprey, we identified not only unusual synaptic patterns and the absence of a connection between the completion of synapsis and the onset of reactivation but also a unique pattern of the distribution of monomethylated histone H3K4. This pattern has yet to be interpreted and indicates that many details of meiotic chromatin epigenetics remain unknown. The question of where some of the identified differences from the published data come from is tricky because currently the data for a large-scale assessment of the functioning of the lampreys' meiotic chromatin is deficient. Nonetheless, we should not forget that jawless taxa split off from the main branch of the vertebrate evolutionary tree (jawed animals) approximately 535–462 million years ago, and considerable evolutionary shifts/modifications of biological processes may have occurred during this long period. Additionally, the identified specific features may be a part of wide variation of epigenetic patterns. Further research will help to clarify and decipher points of difference and similarity. Lamprey meiosis represents a new prism through which many more discoveries may be detected.

Supplementary Materials: The following supporting information can be downloaded at: www.mdpi.com/xxx/s1, Figure S1: Electron microscopic microphotos of lamprey spermatocytes at the pachytene stage; Figure S2: Immunolocalization of SYCP3 and RNA polymerase (RNAPII) proteins in lamprey spermatocytes at the prophase I; Figure S3: Immunocalization of SYCP3 and

RNA polymerase (RNAPII) proteins in lamprey spermatocytes at the zygotene and pachytene stages; Figure S4: Immunolocalization of SYCP3 and H3K4me1 proteins in lamprey spermatocytes at different stages of prophase I; Figure S5: Immunolocalization of SYCP3 and H3K4me1 proteins in lamprey spermatocytes at different stages of prophase I; Figure S6: Immunolocalization of SYCP3 and H3K4me1 proteins in lamprey spermatocytes at different stages of prophase I.

Author Contributions: Conceptualization, S.M. and N.T.; methodology, S.M. and O.K.; investigation, S.M., N.T. and A.K.; writing, S.M. and O.K.; visualization, S.M.; funding acquisition, S.M. and O.K.; supervision, O.L. All authors have read and agreed to the published version of the manuscript.

Funding: This research was supported by the VIGG RAS State Assignment Contracts, Nos 0092-2022-0002.

Institutional Review Board Statement: Animals were treated according to the Guidelines for Humane Endpoints for Animals Used in Biomedical Research. All the experimental protocols were approved by the Ethics Committee of Vavilov Institute of General Genetics RAS (order No. 3 of 10 November 2016) in accordance with the Regulations for Laboratory Practice in the Russian Federation. All efforts were made to minimize animal suffering.

Informed Consent Statement: not applicable.
Data Availability Statement: not applicable

Acknowledgments: We thank the Genetic Polymorphisms Core Facility of the Vavilov Institute of General Genetics of the Russian Academy of Sciences for the possibility to use microscopes. We are grateful to G.N. Davidovich, A.G. Bogdanov and their colleagues of the Electron Microscopy Laboratory of Biological Faculty of Moscow State University for the technical assistance.

Conflicts of Interest: The authors declare no conflict of interest. The funders had no role in the design of the study; in the collection, analyses, or interpretation of data; in the writing of the manuscript; or in the decision to publish the results.

References

1. Bogdanov, Y.F.; Kolomiets, O.L. Synaptonemal Complex as an Indicator of the Dynamics of Meiosis and Chromosome Variation; KMK Press: Moscow, Russia, 2007; p. 359.
2. Loidl, J. Conservation and variability of meiosis across the eukaryotes. Annu. Rev. Genet. 2016, 50, 293-316. doi: 10.1146/annurev-genet-120215-035100
3. Alavattam, K.G.; Maezawa, S.; Sakashita, A.; Khoury, H.; Barski, A.; Kaplan, N.; Namekawa, S.H. Attenuated chromatin compartmentalization in meiosis and its maturation in sperm development. Nat. Struct. Mol. Biol. 2019, 26, 175-184. doi: 10.1038/s41594-019-0189-y
4. Berrios, S. Nuclear architecture of mouse spermatocytes: chromosome topology, heterochromatin, and nucleolus. Cytogent. Genome Res. 2017, 151, 61-71. doi: 10.1159/000460811
5. Zetka, M.; Paouneskou, D.; Jantsch, V. The nuclear envelope, a meiotic jack-of-all-trades. Cur. Opin. Cell Biol. 2020, 64, 34-42. doi: 10.1016/j.ceb.2019.12.010
6. Matveevsky, S.; Tretiakov, A.; Kashintsova, A.; Bakloushinskaya, I.; Kolomiets, O. Meiotic nuclear architecture in distinct mole vole hybrids with Robertsonian translocations: chromosome chains, stretched centromeres, and distorted recombination. IJMS 2020, 21, 7630. doi: 10.3390/ijms21207630
7. Fallahi, M.; Getun, I.V.; Wu, Z.K.; Bois, P.R. A global expression switch marks pachytene initiation during mouse male meiosis. Genes 2010, 1, 469-83. doi: 10.3390/genes1030469
8. Ball, R.L.; Fujiwara, Y.; Sun, F.; Hu, J.; Hibbs, M.A.; Handel, M.A.; Carter, G.W. Regulatory complexity revealed by integrated cytological and RNA-seq analyses of meiotic substages in mouse spermatocytes. BMC Genomics 2016, 17, 1-7. doi: 10.1186/s12864-016-2865-1
9. da Cruz, I.; Rodríguez-Casuriaga, R.; Santiñaque, F.F.; Farías. J.; Curti, G.; Capoano, C.A.; Folle, G.A.; Benavente, R.; Sotelo-Silveira, J.R.; Geisinger, A. Transcriptome analysis of highly purified mouse spermatogenic cell populations: gene expression signatures switch from meiotic-to postmeiotic-related processes at pachytene stage. BMC Genomics 2016,17, 1-9. doi: 10.1186/s12864-016-2618-1
10. Fine, A.D.; Ball, R.L.; Fujiwara, Y.; Handel, M.A.; Carter, G.W. Uncoupling of transcriptomic and cytological differentiation in mouse spermatocytes with impaired meiosis. Mol. Biol. Cell 2019, 30, 717-728. doi: 10.1091/mbc.E18-10-0681
11. Khalil, A.M.; Driscoll, D.J. Epigenetic regulation of pericentromeric heterochromatin during mammalian meiosis. Cytogent. Genome Res. 2010, 129, 280-289. doi: 10.1159/000315903

12. Page, J.; De La Fuente, R.; Manterola, M.; Parra, M.T.; Viera, A.; Berríos, S., Fernández-Donoso, R.; Rufas, J.S. Inactivation or non-reactivation: what accounts better for the silence of sex chromosomes during mammalian male meiosis? Chromosoma 2012, 121, 307-326. doi: 10.1007/s00412-012-0364-y
13. de la Fuente, R.; Pratto, F.; Hernández-Hernández, A.; Manterola, M.; López-Jiménez, P.; Gómez, R.; Page, J. Epigenetic Dysregulation of Mammalian Male Meiosis Caused by Interference of Recombination and Synapsis. Cells 2021, 10, 2311. doi: 10.3390/cells10092311
14. Wang, L.; Xu, Z.; Khawar, M.B.; Liu, C.; Li, W. The histone codes for meiosis. Reproduction 2017, 154, R65-R79. doi: 10.1530/REP-17-0153
15. Turner, J.; Mahadevaiah, S.K.; Fernandez-Capetillo, O.; Nussenzweig, A.; Xu, X.; Deng, C.X.; Burgoyne, P.S. Silencing of unsynapsed meiotic chromosomes in the mouse. Nat. Genet. 2005, 37, 41-47. doi: 10.1038/ng1484
16. Rogakou, E.P.; Pilch, D.R.; Orr, A.H.; Ivanova, V.S.; Bonner, W.M. DNA double-stranded breaks induce histone H2AX phosphorylation on serine 139. J. Biol. Chem. 1998, 273, 5858–5868. doi: 10.1074/jbc.273.10.5858
17. Mahadevaiah, S.K.; Turner, J.; Baudat, F.; Rogakou, E.P.; de Boer, P.; Blanco-Rodríguez, J., Jasin, M.; Keeney, S.; Bonner, W.M.; Burgoyne, P.S. Recombinational DNA double-strand breaks in mice precede synapsis. Nat. Genet. 2001, 27, 271-276. doi: 10.1038/85830
18. Fernandez-Capetillo, O.; Lee, A.; Nussenzweig, M.; Nussenzweig, A. H2AX: the histone guardian of the genome. DNA Repair (Amst) 2004, 3, 959–967. doi: 10.1016/j.dnarep.2004.03.024
19. Manterola, M.; Brown, T.M.; Oh, M.Y.; Garyn, C.; Gonzalez, B.J.; Wolgemuth, D.J. BRDT is an essential epigenetic regulator for proper chromatin organization, silencing of sex chromosomes and crossover formation in male meiosis. PLoS Genet. 2018, 14, e1007209. doi: 10.1371/journal.pgen.1007209
20. Quintella, B.R.; Clemens, B.J.; Sutton, T.M.; Lança, M.J.; Madenjian, C.P.; Happel, A.; Harvey, C.J. At-sea feeding ecology of parasitic lampreys. J. Great Lakes Res. 2021, 47, S72-S89. doi: 10.1016/j.jglr.2021.07.008
21. Janvier, P. Early Vertebrates; Clarendon Press: Oxford, 1996; 393 pp.
22. Hedges, S.B. Molecular evidence for the early history of living vertebrates. In: Major Events in Early Vertebrate Evolution: Paleontology, Phylogeny, Genetics and Development; Ahlberg, P.E., ed.; Taylor and Francis: London, United Kingdom, New York, USA, 2001; pp. 119-134.
23. Janvier, P. Modern look for ancient lamprey. Nature 2006, 443, 921-923. doi: 10.1038/443921a
24. Gess, R.W.; Coates, M.I.; Rubidge, B.S. A lamprey from the Devonian period of South Africa. Nature 2006, 443, 981- 984. doi: 10.1038/nature05150
25. Bayramov, A.V.; Ermakova, G.V.; Kucheryavyy, A.V.; Meintser, I.V.; Zaraisky, A.G. Lamprey as Laboratory Model for Study of Molecular Bases of Ontogenesis and Evolutionary History of Vertebrata. J. Ichthyol. 2022, 1-17. doi: 10.1134/S0032945222060029
26. Timoshevskiy, V.A.; Lampman, R.T.; Hess, J.E.; Porter, L.L.; Smith, J.J. Deep ancestry of programmed genome rearrangement in lampreys. Develop. Biol. 2017, 429, 31-34. doi: 10.1016/j.ydbio.2017.06.032
27. Timoshevskiy, V.A.; Timoshevskaya, N.Y.; Smith, J.J. Germline-specific repetitive elements in programmatically eliminated chromosomes of the sea lamprey (Petromyzon marinus). Genes 2019, 10, 832. doi: 10.3390/genes10100832
28. Nagao, K.; Otsuzumi, T.; Chinone, H.; Sasaki, T.; Yoshimoto, J.; Matsuda, M.; Kubota, S.; Goto, Y. Novel selectively amplified DNA sequences in the germline genome of the Japanese hagfish, Eptatretus burgeri. Sci Rep 2022, 12, 21373. https://doi.org/10.1038/s41598-022-26007-2
29. Peters, A.H.F.M.; Plug, A.W.; van Vugt, M.J.; de Boer, P. A drying-down technique for the spreading of mammalian meiocytes from the male and female germ line. Chromosome Res. 1997, 5, 66 -71. doi: 10.1023/a:1018445520117
30. Page, J.; Berríos, S.; Rufas, J.S.; Parra, M.T.; Suja, J.Á.; Heyting, C.; Fernández-Donoso, R. The pairing of X and Y chromosomes during meiotic prophase in the marsupial species Thylamys elegans is maintained by a dense plate developed from their axial elements. J. Cell Sci. 2003, 116, 551-560. doi: 10.1242/jcs.00252
31. Kolomiets, O.; Matveevsky, S.; Bakloushinskaya, I. Sexual dimorphism in prophase I of meiosis in the Northern mole vole (Ellobius talpinus Pallas, 1770) with isomorphic (XX) chromosomes in males and females. Comp. Cytogenet. 2010, 4, 55. doi: 10.3897/compcytogen.v4i1.25
32. Matveevsky, S.; Bakloushinskaya, I.; Kolomiets, O. Unique sex chromosome systems in Ellobius: How do male XX chromosomes recombine and undergo pachytene chromatin inactivation? Sci. Rep. 2016, 6, 29949, doi:10.1038/srep29949.
33. Matveevsky, S.; Chassovnikarova, T.; Grishaeva, T.; Atsaeva, M.; Malygin, V.; Bakloushinskaya, I.; Kolomiets, O. Kinase CDK2 in mammalian meiotic prophase I: screening for hetero-and homomorphic sex chromosomes. IJMS 2021, 22, 1969. doi: 10.3390/ijms22041969
34. Dresser, M.E.; Moses, M.J. Synaptonemal complex karyotyping in spermatocytes of the Chinese hamster (Cricetulus griseus). Chromosoma 1980, 76, 1-22. doi: 10.1007/BF00292222
35. Van Eenennaam, A.L.; Murray, J.D.; Medrano, J.F. Synaptonemal complex analysis in spermatocytes of white sturgeon, Acipenser transmontanus Richardson (Pisces, Acipenseridae), a fish with a very high chromosome number. Genome 1998, 41, 51-61. doi: 10.1139/g97-101
36. Cheng, J.; Blum, R.; Bowman, C.; Hu, D.; Shilatifard, A.; Shen, S.; Dynlacht, B.D. A role for H3K4 monomethylation in gene repression and partitioning of chromatin readers. Mol. Cell 2014, 53, 979-992. doi: 10.1016/j.molcel.2014.02.032

37. Robinson, E.S.; Potter, I.C. Meiotic chromosomes of Mordacia praecox and a discussion of chromosome numbers in lampreys. Copeia 1969, 4, 824-828. doi: 10.2307/1441804
38. Robinson, E.S.; Potter, I.C. The chromosomes of the southern hemispheric lamprey, Geotria australis Gray. Experientia 1981, 37, 239-240. doi: 10.1007/BF01991630
39. Covelo-Soto, L.; Morán, P.; Pasantes, J. J.; Pérez-García, C. Cytogenetic evidences of genome rearrangement and differential epigenetic chromatin modification in the sea lamprey (Petromyzon marinus). Genetica 2014, 142, 545-554. doi: 10.1007/s10709-014-9802-5
40. Roeder, G.S.; Bailis, J.M. The pachytene checkpoint. Trend. Genet. 2000, 16, 395-403. doi: 10.1016/s0168-9525(00)02080-1
41. Burgoyne, P.S.; Mahadevaiah, S.K.; Turner, J.M.A. The consequences of asynapsis for mammalian meiosis. Nat. Rev. Genet. 2009, 10, 207-216. doi: 10.1038/nrg2505
42. Bhattacharyya, T.; Gregorova, S.; Mihola, O.; Anger, M.; Sebestova, J.; Denny, P., Simecek, P.; Forejt, J. Mechanistic basis of infertility of mouse intersubspecific hybrids. PNAS 2013, 110, E468-E477. doi: 10.1073/pnas.1219126110
43. Jan, S.Z.; Jongejan, A.; Korver, C.M.; van Daalen, S.K.; van Pelt, A.M.; Repping, S.; Hamer, G. Distinct prophase arrest mechanisms in human male meiosis. Development 2018, 145, doi: 10.1242/dev.160614
44. Solari, A.J. Sex chromosome pairing and fertility in the heterogametic sex of mammals and birds, In: Fertility and Chromosome Pairing: Recent Studies in Plants and Animals; Gillies, C.B., ed.; CRC Press, Boca Raton, USA, 1989; pp. 77-107.
45. Spangenberg, V.; Arakelyan, M.; Galoyan, E.; Matveevsky, S.; Petrosyan, R.; Bogdanov, Y.; Danielyan, F.; Kolomiets, O. Reticulate evolution of the rock lizards: meiotic chromosome dynamics and spermatogenesis in diploid and triploid males of the genus Darevskia. Genes 2017, 8, 149. doi: 10.3390/genes8060149
46. Li, X.C.; Barringer, B.C.; Barbash, D.A. The pachytene checkpoint and its relationship to evolutionary patterns of polyploidization and hybrid sterility. Heredity 2009, 102, 24-30. doi: 10.1038/hdy.2008.84
47. Timoshevskiy, V.A.; Herdy, J.R.; Keinath, M.C.; Smith, J.J. Cellular and molecular features of developmentally programmed genome rearrangement in a vertebrate (sea lamprey: Petromyzon marinus). PLoS Genet. 2016, 12, e1006103. doi: 10.1371/journal.pgen.1006103
48. Schimenti, J. Synapsis or silence. Nat. Genet. 2005, 37, 11-13. doi: 10.1038/ng0105-11
49. Selth, L.A.; Sigurdsson, S.; Svejstrup, J.Q. Transcript elongation by RNA polymerase II. An. Rev. Biochem. 2010, 79, 271-293. doi: 10.1146/annurev.biochem.78.062807.091425
50. Eick, D.; Geyer, M. The RNA polymerase II carboxy-terminal domain (CTD) code. Chem. Rev. 2013, 113, 8456-8490. doi: 10.1021/cr400071f
51. Corden, J.L. RNA polymerase II C-terminal domain: tethering transcription to transcript and template. Chem. Rev. 2013, 113, 8423-8455. doi: 10.1021/cr400158h
52. Matveevsky, S.N.; Pavlova, S.V.; Atsaeva, M.M.; Searle, J.B.; Kolomiets, O.L. Dual mechanism of chromatin remodeling in the common shrew sex trivalent (XY1Y2). Comp. Cytogenet. 2017, 11, 727. doi: 10.3897/CompCytogen.v11i4.13870
53. Gil-Fernández, A.; Matveevsky, S.; Martín-Ruiz, M.; Ribagorda, M.; Parra, M.T.; Viera, A., Rufas, J.S.; Kolomiets, O.; Bakloushinskaya, I.; Page, J. Sex differences in the meiotic behavior of an XX sex chromosome pair in males and females of the mole vole Ellobius tancrei: turning an X into a Y chromosome? Chromosoma 2021, 130(2), 113-131. doi: 10.1007/s00412-021-00755-y
54. Viera, A.; Parra, M.T.; Rufas, J.S.; Page, J. Transcription reactivation during the first meiotic prophase in bugs is not dependent on synapsis. Chromosoma 2017, 126, 179-194. doi: 10.1007/s00412-016-0577-6
55. Bae, S.; Lesch, B.J. H3K4me1 distribution predicts transcription state and poising at promoters. Front. Cell Dev. Biol. 2020, 8, 289. doi: 10.3389/fcell.2020.00289
56. Prakash, K.; Fournier, D.; Redl, S.; Best, G.; Borsos, M.; Tiwari, V.K.; Tachibana-Konwalski, K.; Ketting, R.F.; Parekh, S.H.; Cremer, C.; Birk, U.J. (2015). Superresolution imaging reveals structurally distinct periodic patterns of chromatin along pachytene chromosomes. PNAS 2015, 112, 14635-14640. doi: 10.1073/pnas.1516928112